INSTRUMENT POINTING, TRACKING AND VIBRATION SUPPRESSION USING ZERO ANNIHILATION PERIODIC CONTROL

David S. Bayard and Dhemetrios Boussalis
Jet Propulsion Laboratory
California Institute of Technology
4800 Oak Grove Drive
Pasadena, CA 91109

ABSTRACT

A new control concept for instrument pointing, tracking and vibration suppression is introduced based on Zero Annihilation Periodic (ZAP) control, In ZAP control, the control gains vary periodically in time, in sharp contrast to conventional controllers whose control gains are fixed in time. The main advantage is that perfect "deadbeat" pointing/tracking and vibration suppression can be achieved - even in the presence of flexible structural elements and non-colocated actuator/sensor hardware. The deadbeat response has clear advantages for optical instruments which must be held steady and precisely pointed during imaging.

The ability of ZAP designs to effectively control noncolocated/nonminimum-phase configurations opens up many new possibilities for high-performance instrument pointing, vibration damping, target tracking, and other advanced optics control applications.

1. INTRODUCTION

Optical instruments must be held steady and pointed precisely during imaging. In order to achieve this, random disturbances and dynamic disturbances must be suppressed. The suppression of random disturbances using feedback is well established [8]. In contrast, dynamic disturbances arise from flexibility in the mechanical support structure, elastic components, spacecraft booms/masts, etc. Dynamic disturbances are often the most difficult to remove since they can involve lightly damped resonances. Hence, in most instrument control designs, no attempt is made to control such disturbances. Instead, it is typical to wait for such vibrations to subside after each retargeting action, and to accept the resulting settling time of the pointing system. In certain applications, this may be perfectly acceptable. However, in other applications (i.e., limited mission time, limited duration imaging opportunities, etc.,), settling times may be unacceptably long. Furthermore, in applications requiring perpetual retargeting or real-time tracking, the system may never completely settle, and such dynamic disturbances impose a fundamental limit on achievable performance.

This paper presents a new method for controlling dynamic disturbances based on Zero Annihilation Periodic (ZAP) control. The main advantage is that perfect "deadbeat" pointing/tracking and vibration suppression can be achieved - even in the presence of flexible structural elements and non-colocated actuator/sensor hardware. The ZAP control law was introduced in Bayard [3] [4] [5] for controlling nonminimum phase systems using stable plant inversion. The general approach is based on the notion of a mathematical

"lifting" in which a serial-to-parallel conversion is performed on the plant input and output signals, and mappings are considered between the vectorized quantities. As a result of using liftings, the ZAP control gains vary periodically in time, in sharp contrast to conventional controllers whose control gains are fixed in time. Bayard's lifting [5] is a generalization of Lozano's lifting [1 1] to the extended horizon case. The generalization to the extended horizon case is crucial for control gain reduction in order to allow practical implementations of the approach.

In the present paper, an overview of extended horizon liftings is given, and the ZAP controller is derived by minimizing a quadratic input cost subject to a deadbeat tracking objective for the lifted system. The resulting ZAP controller is then demonstrated on problems of instrument pointing, tracking, and vibration suppression.

2. BACKGROUND AND NOTATION

Consider the input/output model,

$$\mathcal{A}(z^{-1})y_\ell = \mathcal{B}(z^{-1})u_\ell \tag{2.1a}$$

$$\mathcal{A}(z^{-1}) = 1 + \sum_{i=1}^{n} a_i z^{-i}; \quad \mathcal{B}(z^{-1}) = \sum_{i=1}^{n} b_i z^{-i} \tag{2.1b}$$

where polynomials A and $\mathcal{B}$ are assumed to be relatively prime. It is assumed that $b_1 \# O$, so that the polynomial $\mathcal{B}$ can be factored uniquely into the form $\mathcal{B}(z^{-1}) = z^{-d} b_1 \bar{\mathcal{B}}(z^{-1})$ where $\bar{\mathcal{B}}(z^{-1})$ is monic and $d = 1$ is the plant delay. It is desired to transform (2.1) into the Block Multirate Input/Output form of Albertos [1], for which it will be necessary to make the following assumptions,

A.1 The plant delay is known (and given by $d = 1$)

A.2 An upper bound $\bar{n} \geq$ n is known on the plant order n

The choice $d = 1$ in assumption A.1 is for convenience only and is not a fundamental restriction. In the case that $d \# 1$, knowledge of d ensures that all subsequent expressions can be appropriately modified without loss of generality.

Choose some horizon time N > $\bar{n}$. The system (2.1) is iterated to give the following system of linear equations,

$$Y(k) = AI\ Y(k) + A_2 Y(k-1) + \&U(k) + B_2 U(k-1) \tag{2.2}$$

where,

$$Y(k) = \begin{bmatrix} y_{kN+1} \\ y_{kN+2} \\ \vdots \\ y_{kN+N} \end{bmatrix}; \quad U(k) = \begin{bmatrix} u_{kN} \\ u_{kN+1} \\ \vdots \\ u_{kN+N-1} \end{bmatrix} \tag{2.3}$$

A_1 = lower triangular Toeplitz, with first column $[0, -a_1, \ldots, -an, 0, \ldots, 0]^T$

A_2 = upper triangular Toeplitz, with first row [0, ...0, –an, ... –al]

B_1 = lower triangular Toeplitz, with first column $[b_1, b_2, \ldots b_n, O, \ldots 0]^T$

B_2 = upper triangular Toeplitz, with first *row [0, ...0,* $b_n, \ldots b_2]$

It is convenient to combine terms involving Y(k) in (2.2) and rearrange to give the following input /out put characterization,

Block Multirate Input/Output (BMIO) Representation

$$\text{Y(k)} = AY(k-1) + HU(k) + BU(k-1) \tag{2.4}$$

where,

$$A = (I - A_1)^{-1} A_2 \tag{2.5a}$$

$$H = (I - A_1)^{-1} B_1 \tag{2.5b}$$

$$B = (I - A_1)^{-1} B_2 \tag{2.5c}$$

Several advantages and properties of the BMIO representation arc discusscdin Albertos [1]. It is noted that since A_1 is lower triangular with zeros on the diagonal, the quantity $(I - A_1)$ is always invertible. Hence the quantities in (2.5) always exist, and the BMIO model (2.4) is a first order vector ARX process which is equivalent to the original system (2.1). It is emphasized that only assumptions A.1 and A.2 were required to put the plant into the desired BMIO form.

Polynomial A is divided into $\mathcal{B}$ to give impulse response sequence $\{h_i\}$,

$$\frac{\mathcal{B}(z^{-1})}{\mathcal{A}(z^{-1})} = \sum_{i=1}^{\infty} h_i z^{-i} \tag{2.6}$$

The quantities *hi* are referred to as Markov parameters. The impulse response sequence {hi} is not assumed to be convergent (i.e., the system may be unstable). Using the Toeplitz structure of *Al* and B_1 and relation (2.6), it can be shown [1][3] that the matrix *H* in (2.4) (2.5b) can be written in terms of the Markov parameters as,

$$H = \begin{vmatrix} h_1 & 0 & \cdots & 0 \\ h_2 & h_1 & \ddots & \vdots \\ \vdots & \ddots & \ddots & 0 \\ h_N & \cdots & h_2 & h_1 \end{vmatrix} \tag{2.7}$$

This is the desired expression for *H,* i.e.,

H = lower triangular Toeplitz, with first column $[h_1, h_2, \ldots . h_N]^T$

Since the delay is unity by assumption (i.e., *d* = 1), the matrix *H* has a nonzero diagonal (i.e., $h_1 \# O$), and is always invertible,

30 GENERALIZED LIFTINGS

In this section, a class of generalized liftings will be defined from the BMIO plant representation (2.4).

Some ncw notation is required at this point. In general, consider some vector $V \in RN$. Then a *partial horizon* vector $V_s = SV$ is defined where $S \in R^{\sigma}$ 'N is a *selection matrix* which selects a $\leq$ N components of V for inclusion in $V_s \in R^{\sigma}$. For this purpose, S will bc a matrix of O's and 1's with a a single "l" in every row, and a single "1" in only σ of its N columns.

As indicated by the expression $V_s = SV$, the subscript "s" will be used throughout to denote quantities which are constructed from "selected" elements of their unsubscripted counterparts.

The selection matrix S defined above can also be thought of as being specified uniquely by a 0,1 *window vector* $\rho = [p_{,}, \ldots . \rho_N]$ whose entries are,

$$\rho_i = \begin{cases} 1 \text{ if } i\text{th entry of } V \text{ is included in } V_s \\ O \text{ otherwise} \end{cases}$$

The number of "l's" in p is defined as u. Note that if the elements of p were to be plotted versus their index, a O, 1 '(window" is formed over the N-step horizon, depicting which σ components of V are to be included in V_s. The construction of S from ρ in this manner defines a one-to-one mapping $S = \mathcal{W}(\rho)$ which will be convenient notation in the paper.

As an example, consider the plot shown in Fig. 1 for an input window ρ_u and an output window ρ_y. The construction of selection matrices S_u and S_y corresponding to the windows ρ_u and ρ_y in Fig. 1, is shown in the example below.

Example 1 Consider the case in Fig. 1 where N = 6, and $\rho_y = [0,0,1,1,1, 0], \rho_u = [0,1,1,1,0,0]$. Then, $\sigma_y = \sigma_u = 3$, $\rho_y^c = [1, 1,0,0,0,1]$ (the *complementary* window to ρ_y) and,

$$S'' = \mathcal{W}(\rho_u) = \begin{bmatrix} 0 & 1 & 0 & 0 & 0 & 0 \\ 0 & 0 & 1 & 0 & 0 & 0 \\ 0 & 0 & 0 & 1 & 0 & 0 \end{bmatrix}_1$$

$$S_y = \mathcal{W}(\rho_y) = \begin{bmatrix} 0 & 0 & 1 & 0 & 0 & 0 \\ 0 & 0 & 0 & 1 & 0 & 0 \\ 0 & 0 & 0 & 0 & 1 & 0 \end{bmatrix}$$

$$S_y^c = \mathcal{W}(\rho_y^c) = \begin{bmatrix} 1 & 0 & 0 & 0 & 0 & 0 \\ 0 & 1 & 0 & 0 & 0 & 0 \\ 0 & 0 & 0 & 0 & 0 & 1 \end{bmatrix}$$

Note that in the example, we have included the selection matrix S_y^c associated with the window ρ_y^c which is defined as the O-1 complement of window ρ_y. This complementary window will play an important role in the following discussion.

Using the above notation, the following partial horizon vectors will be used in the paper,

$$Y_s(k) \triangleq S_y Y(k); \quad S_y \triangleq \mathcal{W}(\rho_y) \in R^{\sigma_y \times N}$$

$$U_s(k) \triangleq S_u U(k); \; S_u \triangleq \mathcal{W}(\rho_u) \in R^{\sigma_u \times N}$$

$$Y_s^c(k) \triangleq S_y^c Y(k); \quad S_y^c \triangleq \mathcal{W}(\rho_y^c) \in R^{(N-\sigma_y)\times N}$$

where ρ_y and ρ_u are specified O, 1 window vectors, and ρ_y^c is defined as the O, 1 complement of ρ_y. Intuitively, Y_s^c is a vector comprised of all elements of the vector Y which arc not included in Y_s.

A general class liftings is now defined from the BMIO plant representation (2.4) by making the input nonzero only over a restricted portion of each horizon. Specifically, as depicted in Fig. 1, the control is chosen as zero outside the window U_s. Using this property, and substituting definitions of U_s, Y_s, and Y_s^c, in the the BMIO model (2.4) gives,

$$\begin{bmatrix} Y(k) \\ U_s(k) \end{bmatrix} = \begin{bmatrix} A & BS_u^T \\ 0 & 0 \end{bmatrix} \begin{bmatrix} Y(k-1) \\ U_s(k-1) \end{bmatrix} + \begin{bmatrix} HS_u^T \\ I \end{bmatrix} U_s(k) \tag{3.1}$$

$$Y_s(k) = [S_y \;\; O] \begin{bmatrix} Y(k) \\ U_s(k) \end{bmatrix} \tag{3.2}$$

It is shown in [3] that the lifted plant (3.1)(3.2) can be transformed by similarity to the following more 'useful form,

Generalized Lifting System Model

$$\begin{bmatrix} Y_s(k) \\ Y_s^c(k) \\ U_s(k) \end{bmatrix} = \begin{bmatrix} S_y A S_y^T & S_y A (S_y^c)^T & S_y B S_u^T \\ S_y^c A S_y^T & S_y^c A (S_y^c)^T & S_y^c B S_u^T \\ 0 & 0 & 1 \end{bmatrix} \begin{bmatrix} Y_s(k-1) \\ Y_s^c(k-1) \\ U_s(k-1) \end{bmatrix} + \begin{bmatrix} S_y H S_u^T \\ S_y^c H S_u^T \\ I \end{bmatrix} U_s(k) \tag{3.3}$$

■

The lifted system model (3.3) is depicted in the block diagram of Fig. 2. It is seen that Y_s and Y_s^c form two coupled subsystems which are driven by a common input U_s.

It is noted that the liftings are defined uniquely by the choice of selection windows ρ_u and ρ_y « An important class of liftings will be defined in the next section.

4. EXTENDED HORIZON LIFTINGS

Consider the class of liftings introduced by Bayard in [5],

Extended Horizon Lifting (OT Form):

$$\rho_u = [\overbrace{0,\ldots,0}^{m},\overbrace{1,\ldots,1}^{\ell},\overbrace{\rho}^{p},\overbrace{1,1,\ldots,1,0,\ldots,0}^{n},\overbrace{0,\ldots,0}^{q}] \quad (4.1a)$$

$$\rho_y = [\overbrace{0,\ldots,0}^{m},\overbrace{0,\ldots,0}^{\ell},\overbrace{\rho}^{p},\overbrace{0,\ldots,0}^{q},\overbrace{0,\ldots,0}^{n-1},\overbrace{1,1,\ldots,1}^{n}] \quad (4.1b)$$

where $m \geq 0$ and $\ell \geq$ O are arbitrary, q = O, $\rho \in R^p$ is an arbitrary (or null) O-1 vector chosen identically in both ρ_u and ρ_y; and n >0 is the order of the irreducible plant (2.1). Furthermore, if the system (2.1) is obtained by a zero-order hold (ZOH) digitization of a continuous-time plant, the integer $q \geq 0$ can be chosen arbitrarily.

Remark 1 Lozano's lifting [11] corresponds to the special case where m = O, ℓ = O, p = 1, $\rho = [0]$, $q = 0$. ■

Remark 2 It is noted that if one chooses m >0 in (4.1), the first control action is not applied until m + 1 sample times into the window. Hence, the extra $m * T$ seconds of free time can be used to perform computations (where T is the sampling interval). Since m can be chosen arbitrarily in this lifting, the dead time can be matched to the real-time computer requirements. ■

Remark 3 If one chooses $\ell > 0$ in (4.1), there are more control inputs than outputs in the lifted system (i.e., $\sigma_u > \sigma_y$). It will be seen that these extra degrees of freedom in the input can be used to advantage to minimize a quadratic control cost and hence reduce control gains significantly compared with the case ℓ = O. ■

It has been shown in [5] that the following conditions are satisfied by the extended horizon lifting (4.1),

Output Tracking (OT) Condition

$$H_s H_s^{\dagger} = I \quad (4.2)$$

Zero Annihilation (ZA) Conditions

$$BS_u^T = \mathbf{o} \quad (4.3a)$$

$$A(S_y^c)^T = O \quad (4.3b)$$

Substituting the 2A conditions (4.3) into (3.3) gives the simplified system model,

Extended Horizon *Lifting System Model*

$$Y_s(k) = S_y A S_y^T Y_s(k-1) + H_s U_s(k) \quad \textbf{(4.4a)}$$

$$Y_s^c(k) = S_y^c A S_y^T Y_s(k-1) + S_y^c H S_u^T U_s(k) \quad (4.4b)$$

where "selected" matrix H_s is defined as,

$$H_s = S_y H S_u^T \tag{4.5}$$

Equivalently, under the 2A conditions the system shown in Fig. 2 simplifies to the system shown in Fig. 3. All of the key properties of the extended horizon lifting (4.1) can be understood by comparing Fig. 2 and Fig. 3. It is noted that Y_s^c no longer couples into the Y_s subsystem. Furthermore, the Y_s^c subsystem has become deadbeat i.e., all of the poles of the Y_s^c subsystem are at the origin. Most importantly, (assuming H_s *is* square), *the transmission zeros of the transfer function from* $U_s(k)$ *to* $Y_s(k)$ *have been annihilated (i.e.,* placed at the origin). If H_s is not square, it is shown in [5] that the transmission zeros of the "squared down" transfer function from *V* (where $U_s = H_s^{\dagger} V$) to Y_s are annihilated.

5. ZERO ANNIHILATION PERIODIC (ZAP) CONTROL

The placement of the transmission zeros to the origin by the extended horizon lifting (4.1) allows stable invertibilit y of the transfer function from *US(k)* to $Y_s(k)$. The ZAP control law which will be discussed next deadbeats the response $Y_s(k)$ to follow the desired $Y_d(k)$, subject to the minimization of a quadratic control cost.

To derive the desired controller, define the output error as,

$$E(k) = Y_d(k) - Y_s(k) \tag{5.1}$$

Substituting (4.4a) into (5. I) gives,

$$E(k) = -S_y A S_y^T Y_s(k-1) - H_s U_s(k) + Y_d(k) \tag{5.2}$$

Consider the problem of forcing the error in (5.1) to zero in a single step, while minimizing a quadratic control cost penalty, i.e.,

$$\min_{U_s(k)} \; U_s^T(k) U_s(k) \tag{5.3}$$

subject to

$$E(k) = O \tag{5.4}$$

In light of the OT condition (4.2), this minimization problem can be solved uniquely to give [5],

Zero *Annihilation Periodic (ZAP) Control Law:*

$$U_s^{\circ}(k) = H_s^{\dagger} \left(-S_y A S_y^T Y_s(k-1) + Y_d(k) \right) \tag{5.5}$$

$$= K^{\circ} Y_s(k-1) + L^{\circ} Y_d(k) \tag{5.6}$$

where the corresponding feedback gains arc defined as,

$$K^\circ = -H_s^\dagger S_y A S_y^T \qquad 5.7a)$$

$$L^\circ = H_s^\dagger \qquad (5.7b)$$

Here the superscript "o" is chosen to emphasize the fact that the control nulls (i.e., dead-beats) the output. Also, in light of the OT condition, H_s has full row rank and onc can write $Ht = H_s^T(H_s H_s^T)^{-1}$ (cf., Barnett [2]).

For convenience the ZAP control law is summarized in the block diagram of Fig. 4. We have the following result.

Lemma 1 *(ZAP Control) Consider the closed-loop system arising from the extended horizon lifting (4. 1) under 2A P control (5. 6). Then,*

(i) The quadratic control *cost* **(5.** *3) is minimized at each stage, subject to the deadbeat tracking constraint* **(5.4),**

(ii) AU closed-loop poles are at the origin (i. e., *the closed-loop response is deadbeat), and hence* $Y_s(k)$ *converges to* $Y_d(k)$ *in a single step,*

(iii) The closed-loop system is *internally stable (e.g.,* $Y_s^c(k)$ remains *bounded).*

Proof: Result (i) follows from the OT condition (4.2) and well known minimum-norm properties of the Moore-Penrose inverse (cf., Barnett [2]). Now form the closed-loop system from the simplified lifted plant (4.4) under ZAP control (5.6),

$$\begin{bmatrix} Y_s(k) \\ Y_s^c(k) \\ U_s(k) \end{bmatrix} = A_{cl} \begin{bmatrix} Y_s(k-1) \\ Y_s^c(k-1) \\ U_s(k-1) \end{bmatrix} + B_{cl} Y_d(k) \qquad ,5 \quad 8 \quad)$$

where,

$$A_{cl} = \begin{bmatrix} (I - H_s H_s^\dagger) S_y A S_y^T & O & 0 \\ S_y^c (I - H S_u^T H_s^\dagger S_y) A S_y^T & O & 0 \\ -H_s^\dagger S_y A S_y^T & 0 & 0 \end{bmatrix}; \quad B_{cl} = \begin{bmatrix} H_s H_s^\dagger \\ S_y^c H S_u^T H_s^\dagger \\ H_s^\dagger \end{bmatrix} \qquad ,5 \quad , \quad)$$

Results (ii) and (iii) follow by substituting the OT condition (4.2) into (5.9), and noting that the resulting closed-loop matrix A_{cl} is stable with all of its eigenvalues at the origin.■

Result (i) of Lemma 1" is important because it indicates that control gains associated with using extended horizon liftings will be significantly reduced as one "extends" the horizon length N. Result (ii) indicates that the response will always be deadbeat, and result (iii) ensures that the complementary output Y_s^c remains '(well behaved") even though it is not being controlled directly.

Remark 4 Instead of deadbeat control, a pole placement scheme can be obtained by modifying the deadbeat constraint (5.4) to become $E(k) = \alpha E(k-1)$ in which case the ZAP control becomes $U_s^\circ(k) = K^\circ Y_s(k-1) + L^\circ Y_d(k) - \alpha L^\circ E(k-1)$. •

5. CASE STUDY

In this section, the ZAP controller is demonstrated on problems of instrument pointing, tracking, and vibration suppression.

5.1 Instrument Model

For demonstration purposes, the instrument under consideration is depicted in Fig. 5. The instrument consists of a main body having mass M with center of mass C_p and a smaller body having mass m with center of mass C_s. It is seen that these bodies are connected by a mast of which extends paraxially, and which may be flexible in practice. The flexibility is modelled by a rotational spring, with stiffness given by k. The center of mass of the entire system is given as C (here the mass of the mast is neglected). As is typically done in practice, the entire system is mounted on a gimbal about its center of mass at location C'. The angle that the main body makes with the local horizontal is denoted as θ_p and the angle the small mass makes with the local horizontal is denoted as θ_s. The equations of motion are given as,

$$\tilde{M}\ddot{x} + \tilde{K}x = \begin{bmatrix} u \\ 0 \end{bmatrix}$$

where u is the control torque about C, x = $[\theta_p, \theta_s, \dot{\theta}_p, \dot{\theta}_s]^T$, and

$$\tilde{M} = \begin{bmatrix} J_p + M\ell_p^2 & 0 \\ 0 & m\ell_s^2 \end{bmatrix}; \quad \tilde{K} = \begin{bmatrix} k & -k \\ -k & k \end{bmatrix}$$

Values for the example are chosen as, M = 333 kg, m = 100 kg, k = 40000 Nm/rad. The inertias are computed as $J_p = M \cdot \frac{2}{3}$ = 222 for the main body assuming a square cross-section with 2-meter sides, and a point mass approximation is made for the smaller mass, The center of mass is computed from the expression (assuming the mass of the mass is negligible), $M\ell_p = m\ell_s$. Specifying the mast length as 2.47 meters gives ℓ_p = .8 meters and ℓ_s = 2,67.

The control objective is to drive θ_p to some desired angle θ_d while ensuring that the vibrations of the mast subside, i.e., $\delta\theta \rightarrow$ O where $\delta\theta = \theta_s - O_p$. Several digital control architectures will be considered. The system is digitized using a zero-order-hold (ZOH) at a sampling period of T = .1 seconds.

5.2 PD Colocated Feedback

First, a simple proportional-derivative (PD) feedback control is considered, using measurements and torque actuation colocated on the main body. The architecture is depicted in Fig. 6. This case will provide a comparison with noncolocated designs. The PD gains are chosen as K_p = 250 and K_d = 1000, using an ad-hoc root-locus/simulation design approach based on minimizing settling time while damping vibrations and satisfying an actuator saturation constraint of $|u| \leq 250$ N-m. The step response is shown in Fig. 7. It is seen that the settling time is approximately 12 seconds, and that the torque constraint is satisfied as desired. It is seen from Fig. 8, that the PD design can just barely support tracking of a staircase trajectory which jumps every 11.4 seconds. Such tracking profiles

arise often in applications requiring scanning regions of space, mosaic reconstruction of planet surfaces, retargeting, etc.

5.3 Noncolocated ZAP Control

As a comparison, a noncolocated ZAP control design is considered next. As depicted in Fig. 9, the ZAP controller is designed using feedback from θ_s which is noncolocated with the main body torque actuator. This gives rise to a nonminimum-phase transfer function from u to θ_s which is generally much harder to control than the minimum-phase transfer function from u to θ_p in the colocated case. For this noncolocated design, an extended horizon lifting of size $N = 57$ is chosen where $m = O$, $\ell = 49$, $p = 0$, $n = 4$, $q = 0$. Here, n has been chosen equal to the plant order as required by (4.1), and the integer ℓ has been adjusted to keep the torque within the allowed limits. Despite the well-known difficulties associated with controlling a noncolocated/nonminimum-phase transfer function, it is seen that the settling time shown in Fig. 10 has been improved to approximately 5 seconds, with the actuator saturation constraint ± 250 Nm still satisfied.

It is noted that in addition to the improvement in settling time in Fig. 10, the actual profile is deadbeat, i.e., aftcr 5 seconds the platform is pointing perfectly and all of the vibrations have died out completely. A deadbeat response has clear advantages for optical instruments which must be held steady and precisely pointed during imaging. In Fig. 11, it is seen that the ZAP controller easily tracks the 11.4 second staircase trajectory that the PD controller of Sect. 5.2 had trouble with. In light of the improved settling time, it is shown in Fig. 12 that the staircase trajectory can be pushed to jump at intervals as short as 5.7 seconds without violating the actuator saturation constraint. In practice, this can amount to a significant savings in retargeting time and overall mission time.

It is also emphasized that since the lifted plant is stably invertible, there is no theoretical limit to how fast the ZAP controller can perform retargeting, and simultaneously dampen vibrations. This is due to the special properties of zero annihilation, and is somewhat remarkable in light of the fact that the unlifted transfer function in this case is noncolocated/nonminimum-phase. A caveat, of course, is that sufficient torque must be available to implement the controller. For example, using an extended horizon lifting of size $N = 18$ where $m = 0$, $\ell = 10$, $p = 0$, $n = 4$, $q = O$, the settling time is reduced to 1.4 seconds. This design shown in Fig. 13, applied to tracking a 3.6 second staircase trajectory. It is seen that due to such fast responses, the peak torque requirements have correspondingly increased to ± 2500 Nm. Note that to avoid actuator saturation for this design it would be necessary to scale down the jumps in the staircase trajectory to 1/10 rad, or to get bigger actuators. Aside from actuator saturation issues, the practical limit on the ZAP controller bandwidth will be determined by such factors as high-frequency parasitic, model uncertainty, and numerical stability associated with using finite arithmetic.

5.4 ZAP Plus PD Control

An important issue is that of suppressing random noise disturbances. Since ZAP control operates *open-loop* within each horizon of length N, it would be ineffective at suppressing random disturbances having correlation length shorter than $N \cdot T$ seconds. When such

disturbances are present, an effective approach is to use the ZAP controller as an outer loop in a two-loop control design where the inner-loop controller is designed specifically to suppress noise. One possible architecture is shown in Fig. 14, where the inner-loop is chosen as the colocated PD controller discussed earlier in Sect. 5.2. Since the PD cent roller is colocatcd, it acts to add broadband damping into the system which helps to reduce the effect of broadband noise on basebody motion.

A digital integrator $z/(z-1)$ has been introduced into the architecture of Fig. 14, so that the ZAP control will go to zero when a steady-state pointing condition is attained. This is needed because the ZAP control cannot sustain a constant force/torque profile in steady-state since part of each input horizon must be zero by definition. It is worth noting that the cascaded plant can no longer be interpreted as the zero-order hold (ZOH) digitization of a continuous-time plant, and hence the usc of an integrator restricts the choice of liftings (4.1) to those for which $q = O$.

For the ZAP outer-loop design, an extended horizon lifting of size $N = 58$ is chosen where m = 0, $\ell = 49, p = 0, n = 5$, $q = 0$, Note that the additional state due to the cascaded integrator now requires the choice n = 5 as the plant order. The step response of the two-loop control design is shown in Fig. 15. It is seen that the settling time is approximately 5 seconds. Hence, the fast response of the deadbeat ZAP controller is retained in the two-loop design, Of course, the main advantage of using the two-loop design over using the ZAP control alone is that the inner-loop PD controller will add damping in the presence of random disturbances. Hence, the two-loop control architecture in Fig, 14 retains the properties of each loop separately.

6. DISCUSSION

The design of a ZAP controller will generally require more accurate model information than the design of a colocated PD controller, This is essentially the price to be paid for controlling noncolocated/nonminimum-phase systems. However, if accurate knowledge is not available, plant parameters can be found using adaptive methods. For example, it is noted that the lifted dynamics (4.4a) are linear-in-the-parameters. Hence, recursive least squares methods can be used to estimate the plant parameters and update the ZAP controller. Alternatively, it is noted that the ZAP control law (5.6) is linear in the control gains K° and Lo. Stable direct adaptive control schemes for this *linear controller form* can be developed based on the ideas in Goodwin and Sin [10], as long as certain modifications are made to ensure that Lo is invertible on its estimate. Details can be found in [6]. Related methods for adaptive periodic control can be found in [4] and [11].

The ZAP control design requires knowledge of the plant order and delay. Since these quantities will generally not be known exactly in a real application, there is some question of robustness of the ZAP controller under mismatched conditions. This remains as a topic for further investigation.

The ZAP design was developed here for single-input single-output systems. The extension ZAP control to multivariable systems is clearly relevant and remains to bc developed further.

While the present paper has focused on the pointing and tracking of an entire instrument,

simulation studies demonstrating ZAP control on the ASTREX structural model can be found in [7] applied to vibration suppression of the secondary mirror using the piezoelectric sensing/actuation embedded in the "smart strut" tripod.

7. CONCLUSIONS

The Zero Annihilation Periodic (ZAP) controller has been applied to the problem of instrument pointing, tracking, and vibration suppression. It is shown that the response from using the ZAP controller is always deadbeat, regardless of whether the plant is minimum or nonminimum-phase. The deadbeat response has clear advantages for optical instruments which must be held steady during critical periods of imaging/photon accumulation, etc.. It was also shown how the ZAP control can be integrated into an inner/outer loop control architecture, providing an effective method to retain a fast settling time while suppressing random noise disturbances.

An important conclusion from the case study example is that a noncolocated ZAP controller can provide a shorter settling time than a colocated PD controller for the same actuator torque constraint. This is somewhat remarkable in light of the fact that the colocated transfer function is minimum-phase while the noncolocated transfer function is non-minimum phase. This example clearly demonstrates the ability of ZAP designs to effectively control noncolocated/nonminimum-phase configurations and opens up many new possibilities for high-performance instrument pointing, vibration damping, target tracking, rastering, control of fast steering mirrors, and other advanced optics control applications.

ACKNOWLEDGEMENTS

This research was performed at the Jet Propulsion Laboratory, California Institute of Technology, under contract with the National Aeronautics and Space Administration.

REFERENCES

[1] P. Albertos, "Block multirate input-output model for sampled-data control systems," IEEE Trans. Automatic Control, vol. 35, no. 9, pp. 1085-1088, September 1990.

[2] S. Barnett, Matrices: *Methods and Applications.* Clarendon Press, Oxford England, 1990.

[3] D.S. Bayard, "Globally stable adaptive periodic control," Jet Propulsion Laboratory, Internal Document JPL D-9448, February 1992.

[4] D.S. Bayard, "Zero annihilation methods for direct adaptive control of nonminimurn-phase systems," in *Proc. Seventh Yale Workshop on Adaptive and Learning Systems,* Yale University, May 1992.

[5] D.S. Bayard, "Extended horizon liftings: Theory and applications," Jet Propulsion Laboratory, Internal Document, JPL D-10616, March 16, 1993; abridged version to appear in IEEE Trans. Automatic Control, 1994.

[6] D.S. Bayard, "Stable adaptation of extended horizon liftings," Jet Propulsion Laboratory, Internal Document, in preparation.

[7] D.S. Bayard, and D. Boussalis, "Noncolocated Structural Vibration Suppression Using Zero Annihilation Periodic Control," 2nd IEEE Conference on Control Applications, Vancouver, Canada, September 1993.

[8] H.W. Bode, *Network Analysis and Feedback A mplifier* Design. New York: Van Nostrand, 1945.

[9] E.J. Davison and S.H. Wang, "Properties and calculation of transmission zeros of linear multivariable systems," Automatic, Vol. 10, pp. 643-658, 1974.

[10] G .C. Goodwin and K.S. Sin, *Adaptive Filtering Prediction and Control.* Prentice-Hall, Englewood Cliffs, New Jersey, 1984.

[11] R. Lozano-Leal, "Robust adaptive regulation without persistent excitation," IEEE Trans. Automatic Control, vol. 34, no. 12, pp. 1260-1267, December 1989.

FIGURES

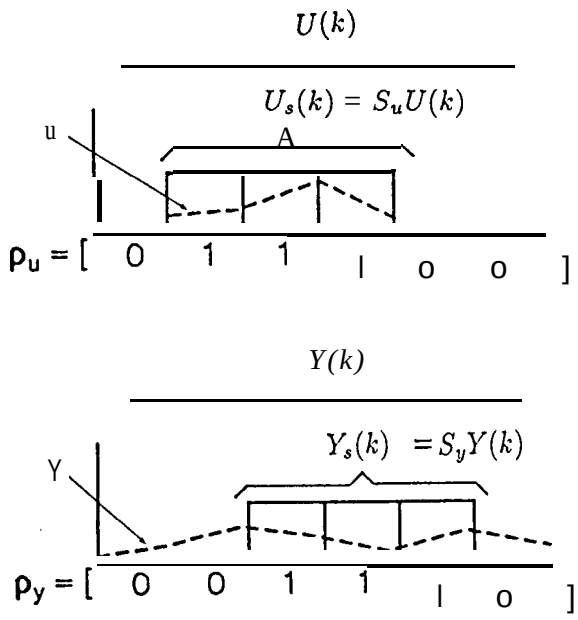

Figure 1: Partial horizon vectors U_s and Y_s defined from windows $p.$ and ρ_y

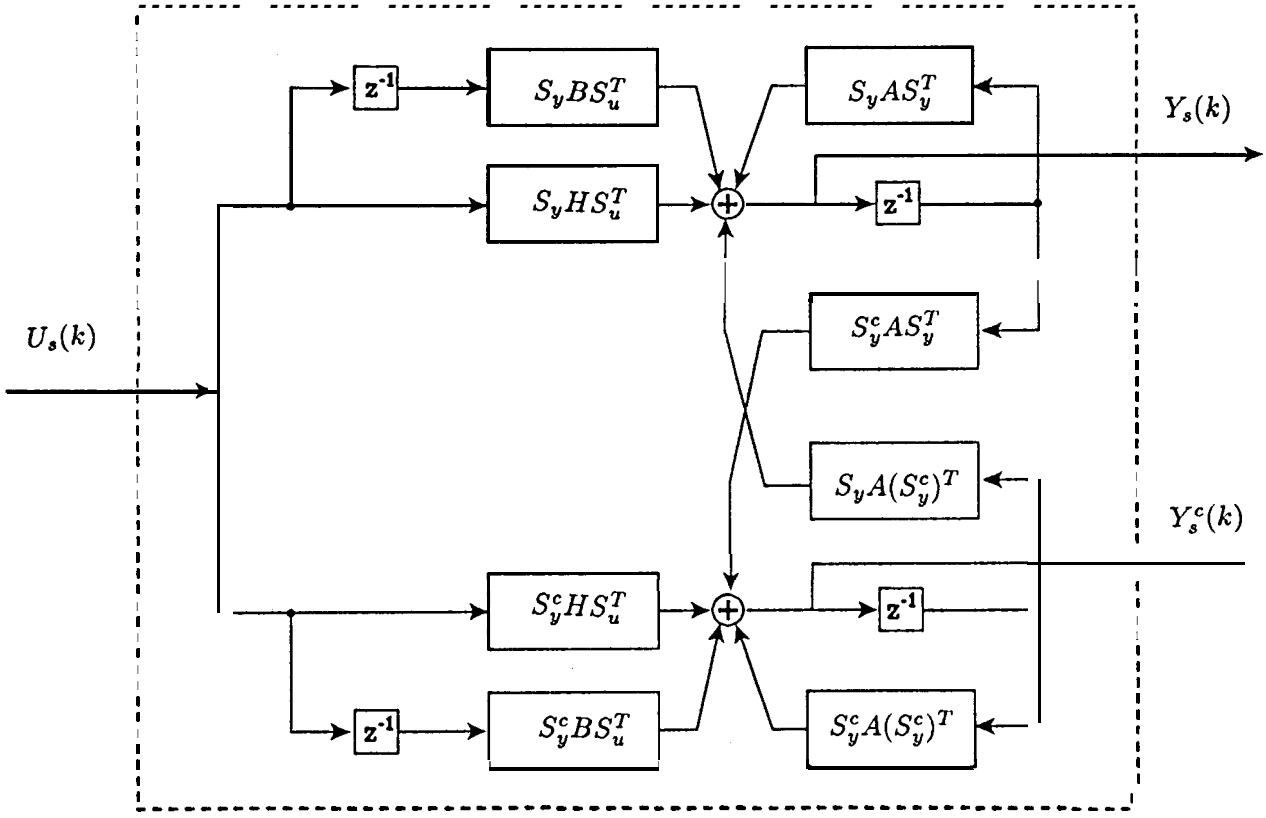

Figure 2: System Model for Generalized Lifting

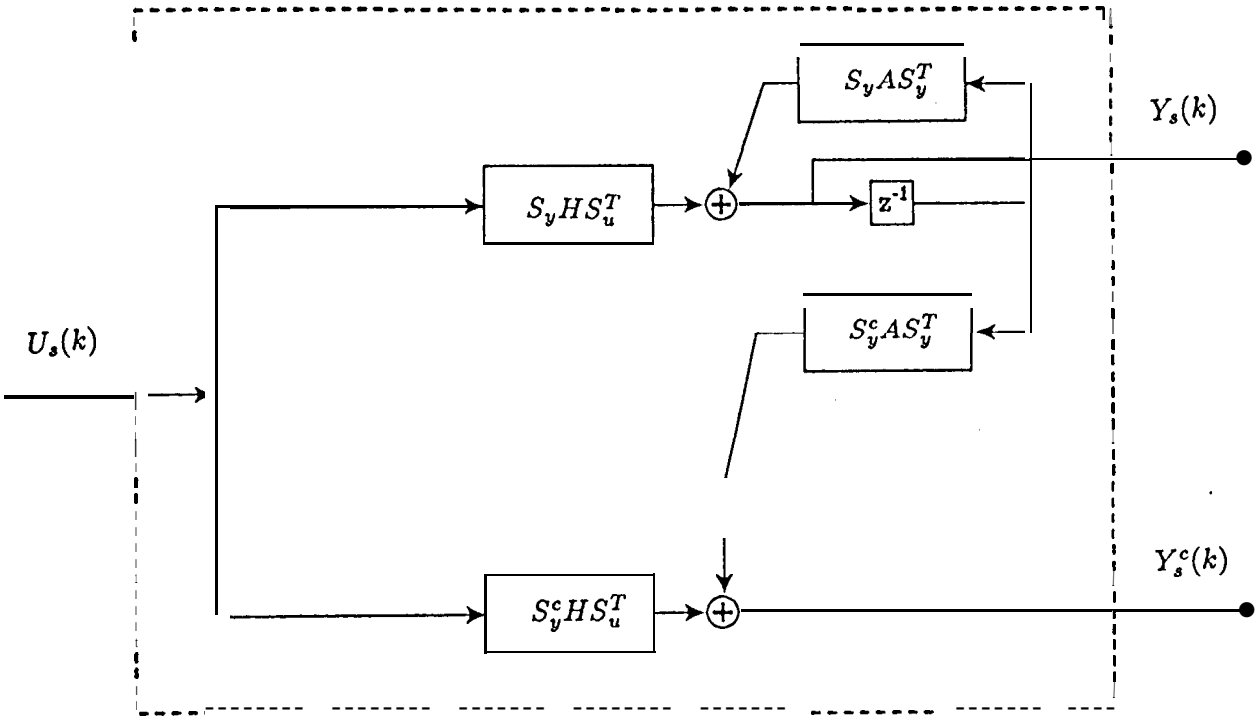

Figure 3: System Model for Extended Horizon Lifting

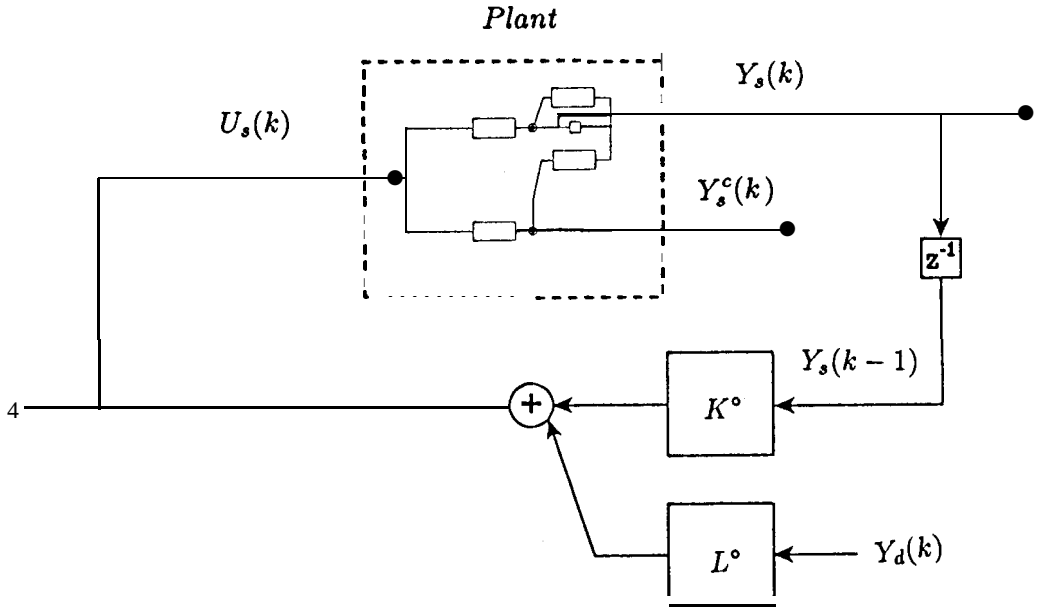

Figure 4: Zero Annihilation Periodic (ZAP) control architecture

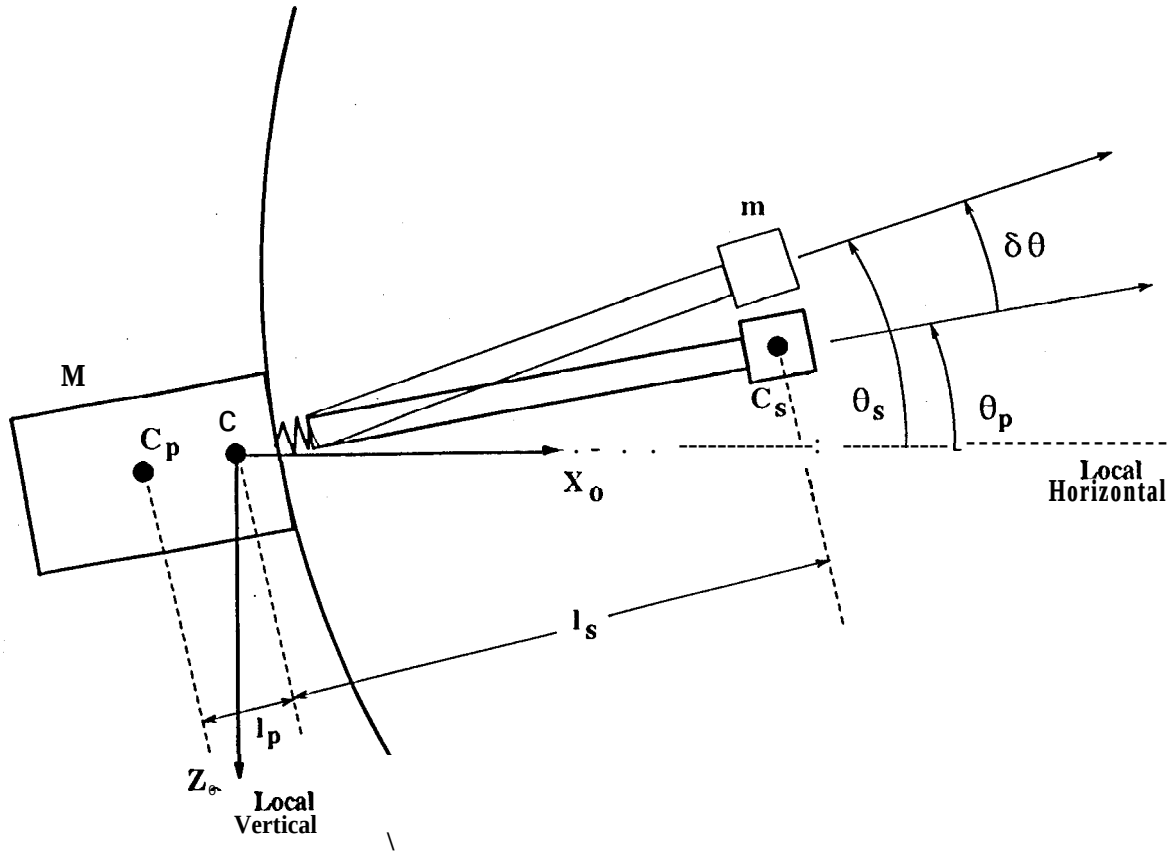

Figure 5: Instrument Model for Case Study

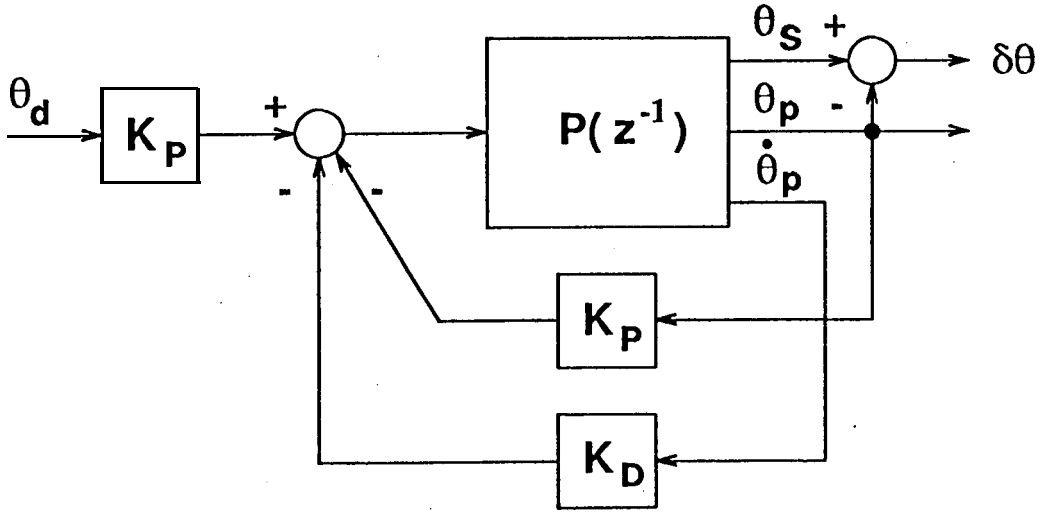

Figure 6: Control architecture using colocated PD feedback

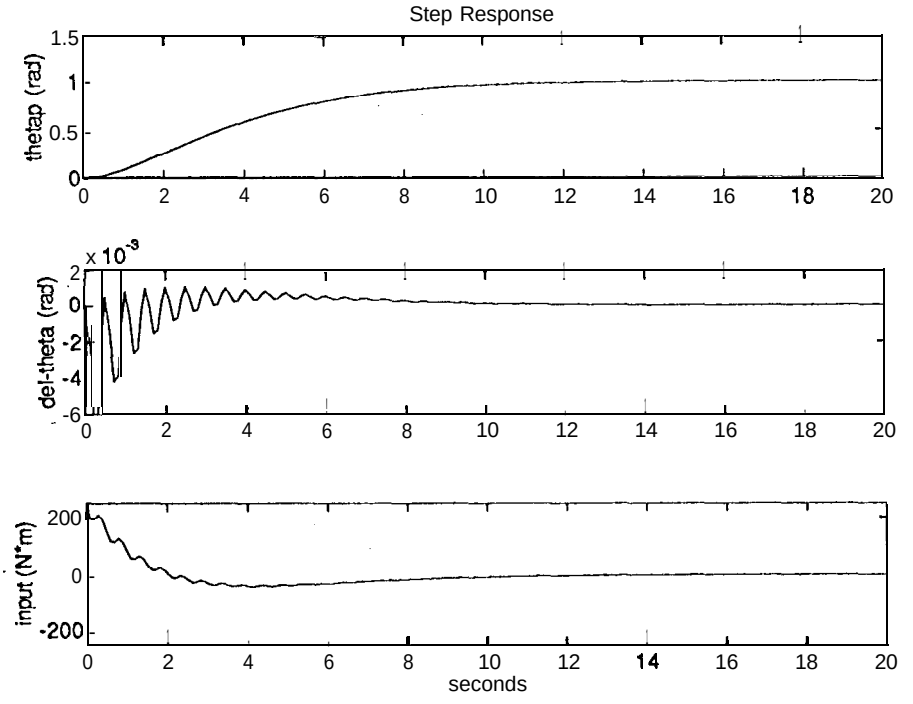

Figure 7: Step response using colocated PD feedback control

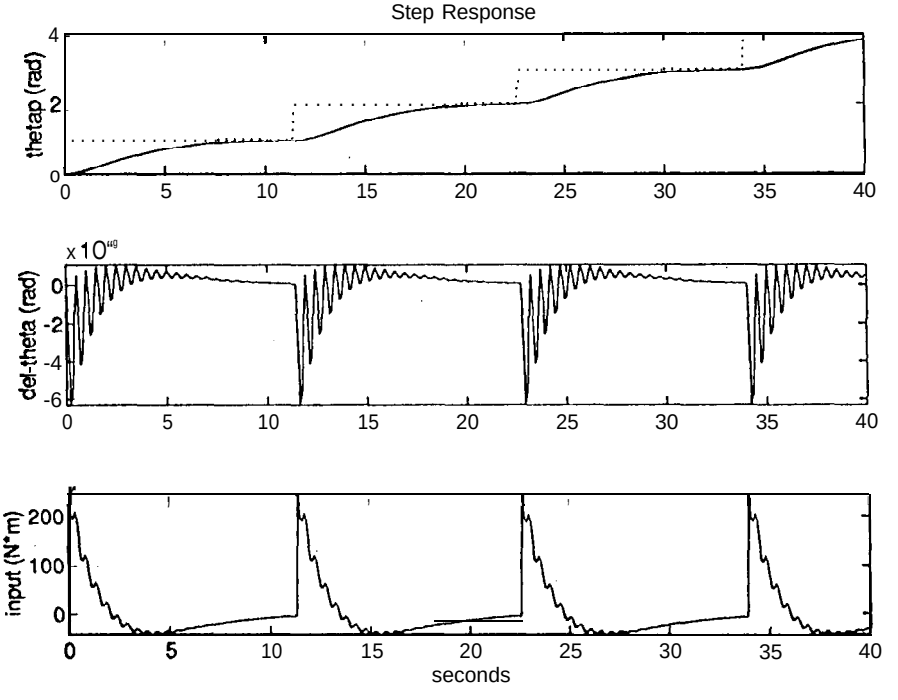

Figure 8: Staircase tracking (11.4 second jumps) using colocated PD feedback control

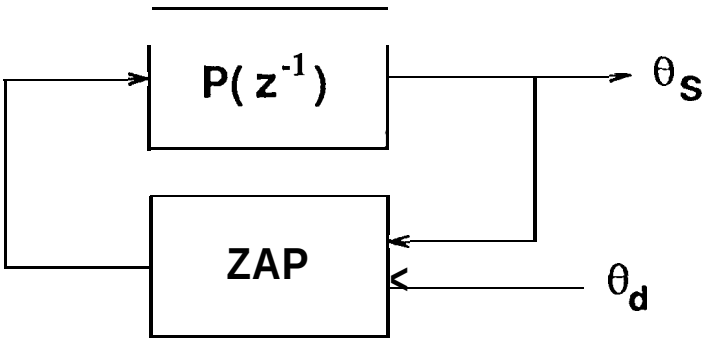

Figure 9: Control architecture using noncolocated ZAP feedback

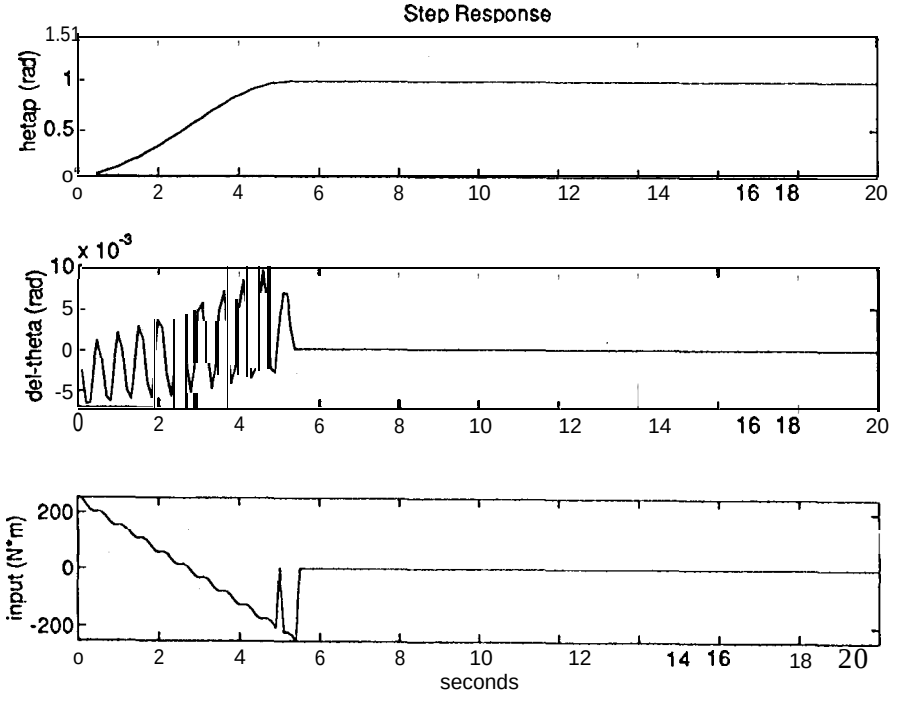

Figure lO: Step response using noncolocated ZAP control

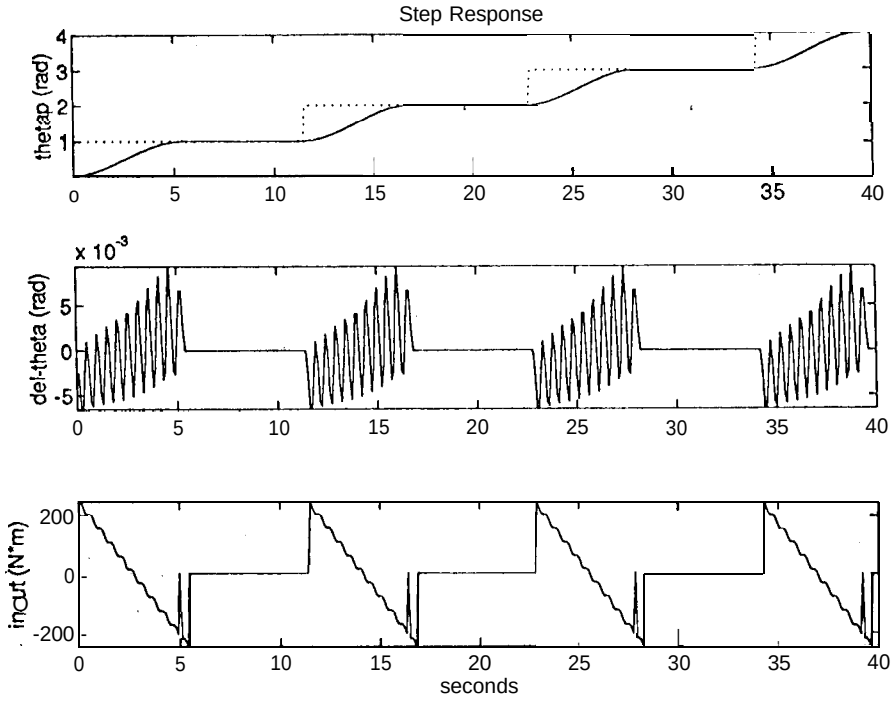

Figure 11: Staircase tracking (11.4 second jumps) using noncolocated ZAP control

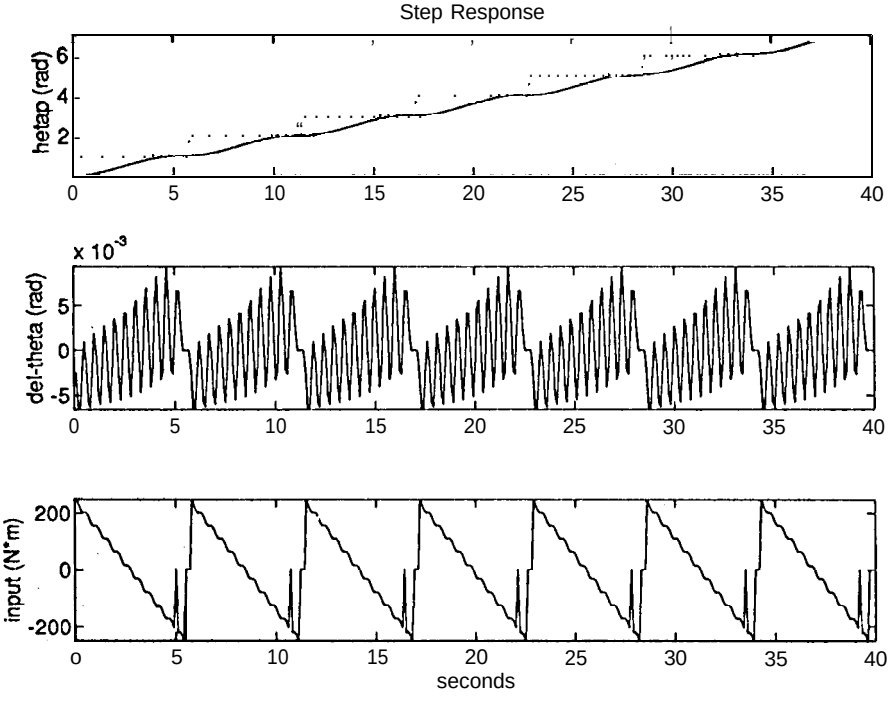

Figure 12: Staircase tracking (5.7 second jumps) using noncolocated ZAP cent rol

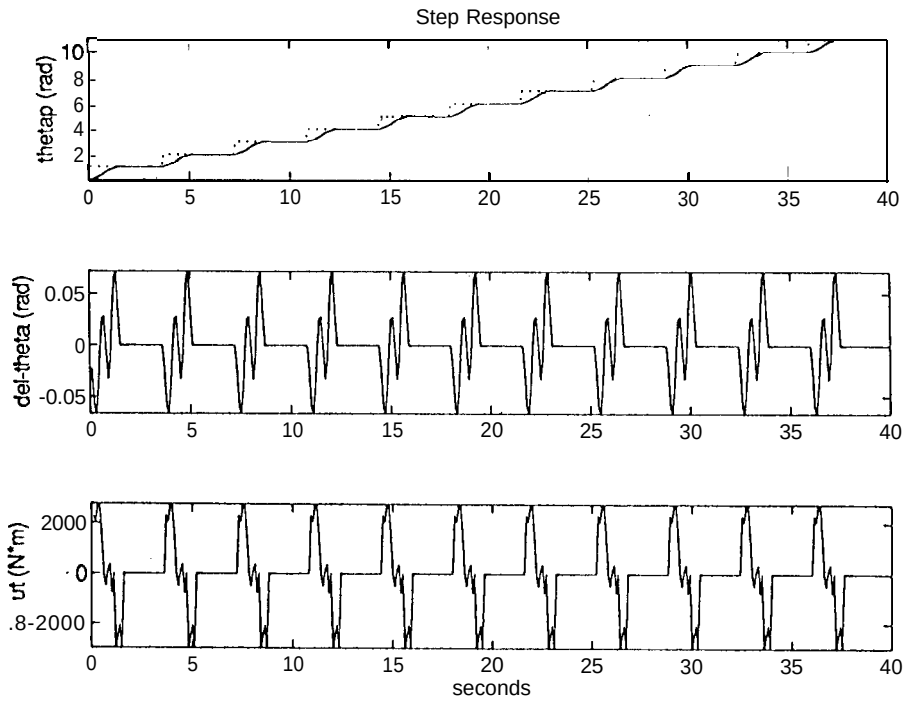

Figure 13: Staircase tracking (3.6 second jumps) using noncolocated ZAP control

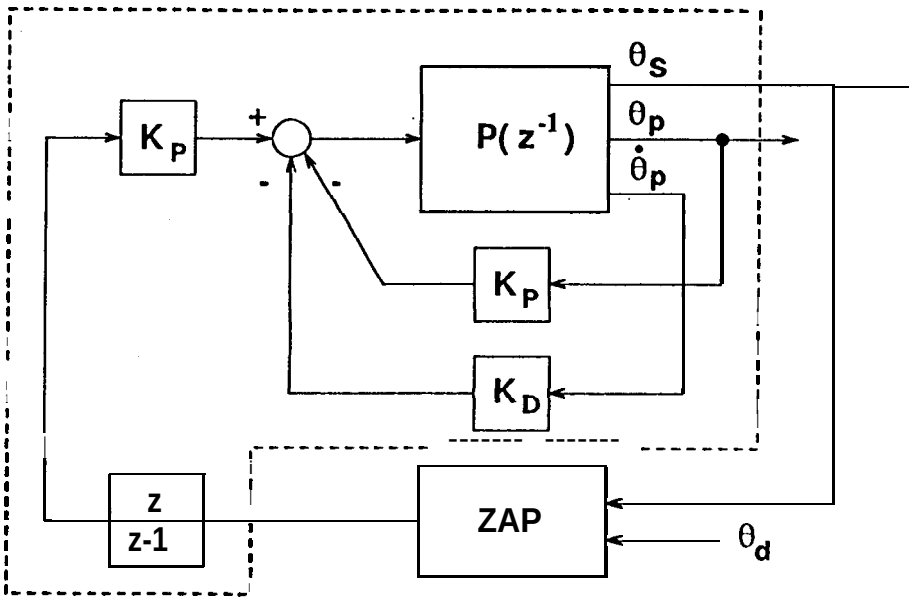

Figure 14: Two-loop control architect ure

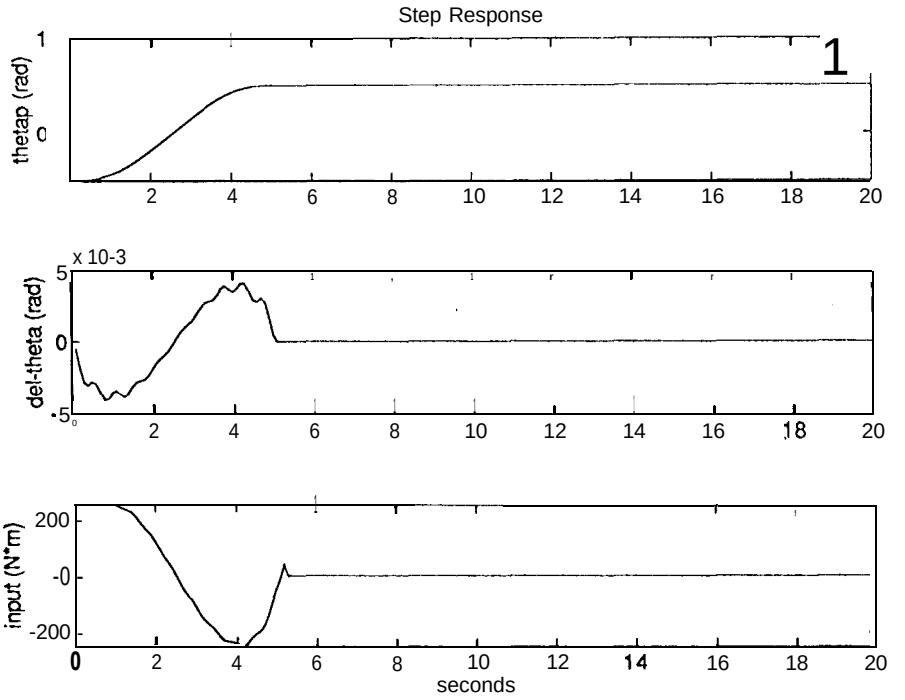

Figure 15: Step response of two-loop control system